Regular Article

blood

PLATELETS AND THROMBOPOIESIS

Cellubrevin/vesicle-associated membrane protein-3–mediated endocytosis and trafficking regulate platelet functions

Meenakshi Banerjee,[1] Smita Joshi,[1] Jinchao Zhang,[1] Carole L. Moncman,[1] Shilpi Yadav,[2] Beth A. Bouchard,[3] Brian Storrie,[2] and Sidney W. Whiteheart[1]

[1]Department of Molecular and Cellular Biochemistry, University of Kentucky, Lexington, KY; [2]Department of Physiology and Biophysics, University of Arkansas for Medical Sciences, Little Rock, AR; and [3]Department of Biochemistry, University of Vermont, Burlington, VT

Key Points

- Platelet VAMP-3 mediates receptor-mediated endocytosis and endocytic trafficking of cargo.
- Platelet VAMP-3 regulates spreading, clot retraction, and TPOR/Janus kinase 2 signaling.

Endocytosis is key to fibrinogen (Fg) uptake, trafficking of integrins ($\alpha IIb\beta_3$, $\alpha_v\beta_3$), and purinergic receptors ($P2Y_1$, $P2Y_{12}$), and thus normal platelet function. However, the molecular machinery required and possible trafficking routes are still ill-defined. To further identify elements of the platelet endocytic machinery, we examined the role of a vesicle-residing, soluble *N*-ethylmaleimide factor attachment protein receptor (v-SNARE) called cellubrevin/vesicle-associated membrane protein-3 (VAMP-3) in platelet function. Although not required for normal platelet exocytosis or hemostasis, VAMP-$3^{-/-}$ mice had less platelet-associated Fg, indicating a defect in Fg uptake/storage. Other granule markers were unaffected. Direct experiments, both in vitro and in vivo, showed that loss of VAMP-3 led to a robust defect in uptake/storage of Fg in platelets and cultured megakaryocytes. Uptake of the fluid-phase marker, dextran, was only modestly affected. Time-dependent uptake and endocytic trafficking of Fg and dextran were followed using 3-dimensional–structured illumination microscopy. Dextran uptake was rapid compared with Fg, but both cargoes progressed through $Rab4^+$, $Rab11^+$, and von Willebrand factor $(VWF)^+$ compartments in wild-type platelets in a time-dependent manner. In VAMP-$3^{-/-}$ platelets, the 2 cargoes showed limited colocalization with Rab4, Rab11, or VWF. Loss of VAMP-3 also affected some acute platelet functions, causing enhanced spreading on Fg and fibronectin and faster clot retraction compared with wild-type. In addition, the rate of Janus kinase 2 phosphorylation, initiated through the thrombopoietin receptor (TPOR/Mpl) activation, was affected in VAMP-$3^{-/-}$ platelets. Collectively, our studies show that platelets are capable of a range of endocytosis steps, with VAMP-3 being pivotal in these processes. (*Blood*. 2017;130(26):2872-2883)

Introduction

Blood platelets respond to vascular damage via activation, adhesion, spreading, and subsequent granule exocytosis.[1] Endocytosis, in contrast, is important for cargo packaging (eg, fibrinogen [Fg]) into granules.[2-4] However, platelet endocytosis could also be critical for actively sensing changes in vascular microenvironments and responding to what is being taken up. This is a more dynamic view of platelets as active surveyors of the vasculature, extending the importance of platelet endocytosis beyond granule biogenesis, and perhaps even beyond hemostasis. The mechanistic underpinnings of endocytosis and its importance in platelets are, however, understudied, in part because of a lack of experimental tools.[5] In this manuscript, we report the characterization of a mouse strain whose platelets are defective in endocytic trafficking of cargo.

Endocytosis refers to cargo uptake and receptor trafficking to and from the plasma membrane through distinct membrane-bound compartments called endosomes. Seminal studies from the 1980s provided the first glimpses into the presence of active endomembrane systems in platelets. Platelets have clathrin-coated vesicles[6,7] and can endocytose several plasma proteins (eg, albumin, immunoglobulin G, Fg, von Willebrand factor [VWF], fibronectin) and translocate them to α-granules.[3,8-11] Notably, both clathrin-dependent and clathrin-independent endocytosis have been reported in platelets.[12] In addition, several platelet surface receptors such as integrin $\alpha IIb\beta_3$ and glycoprotein Ib are internalized and then recycled back to the plasma membrane.[13-16] Platelet CLEC-2 is internalized in a Syk-independent manner, whereas Arrestin-2 and Arf6 play crucial roles in endocytic trafficking of the $P2Y_{12}$ receptors.[17,18] ADP and thrombin stimulation leads to translocation of internal pools of receptors and their surface redistribution.[15,19-21] Consistent with these reports of platelet endocytosis, platelets contain key endocytic proteins and regulators, including the vesicle-scission-inducing GTPase, dynamin, dynamin-related protein 1, and adaptor proteins such as disabled-2.[22-27] Recently, we highlighted the role of adenosine 5′-diphosphate (ADP)-ribosylation factor 6 (Arf6), a small GTP-binding protein, that specifically regulates $\alpha IIb\beta_3$-mediated Fg uptake/storage, and hence modulates acute platelet functions such as clot retraction and spreading.[28] These studies are further supported by "omics" analyses,[29,30] which highlight the burgeoning importance and complexity of endocytosis in platelets.

Submitted 9 February 2017; accepted 14 September 2017. Prepublished online as *Blood* First Edition paper, 20 September 2017; DOI 10.1182/blood-2017-02-768176.

The online version of this article contains a data supplement.

There is an Inside *Blood* Commentary on this article in this issue.

The publication costs of this article were defrayed in part by page charge payment. Therefore, and solely to indicate this fact, this article is hereby marked "advertisement" in accordance with 18 USC section 1734.

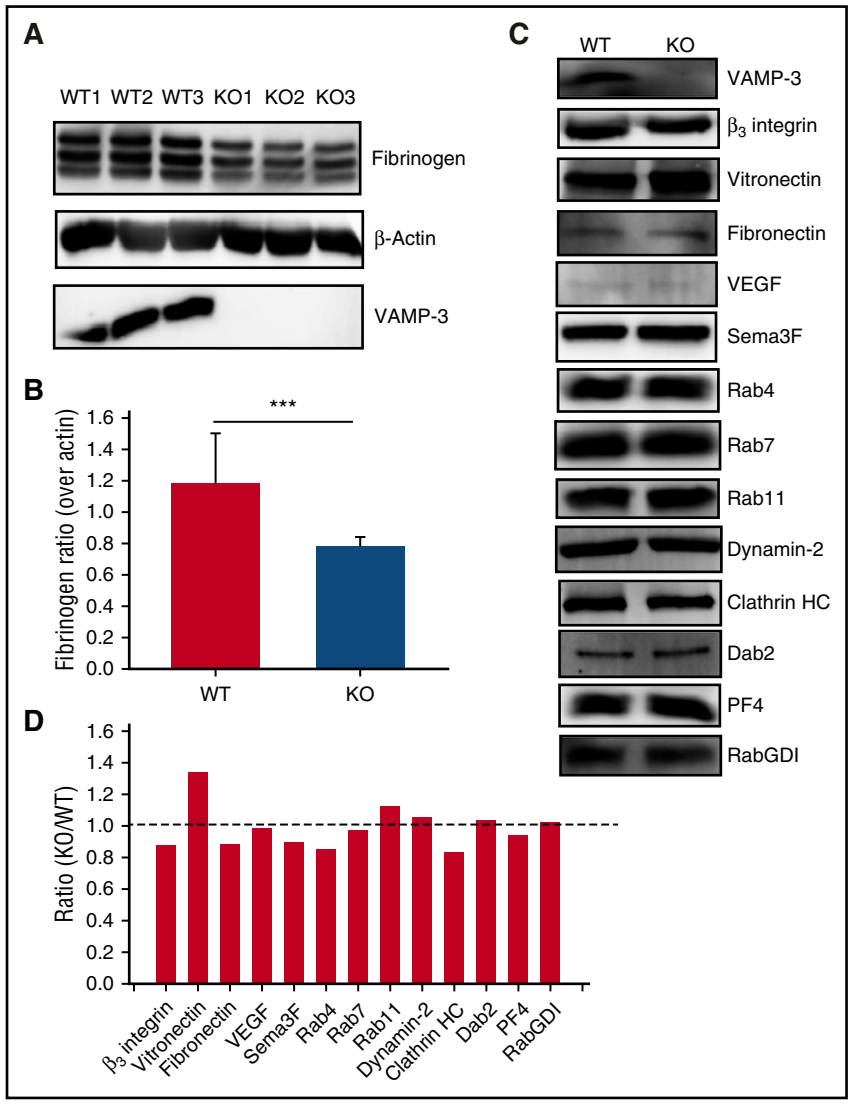

Figure 1. VAMP-3$^{-/-}$ platelets had lower fibrinogen levels. (A) Fg levels in washed platelet extracts from WT and VAMP-3$^{-/-}$ mice (3 each) were measured by western blotting. β-actin was used as loading control. (B) Quantification of Fg levels in panel A was performed using ImageQuantTL and plotted with SigmaPLot software (v13.0). (C) Comparison of protein levels by western blotting between WT and VAMP-3$^{-/-}$ platelets. Washed platelet extracts (5×10^7 platelets/lane) were loaded, and the indicated proteins were probed by western blotting. (D) Quantification of protein levels was performed using ImageQuantTL, and data were plotted as the ratio of VAMP-3$^{-/-}$ over WT. The dashed line represents the ratio 1 of KO/WT protein levels. Statistical analyses were done using Student *t* test; ***$P \leq .001$. Data for panels C and D are representative of platelets pooled from 2 to 3 mice in at least 2 independent experiments.

Here we describe a role for cellubrevin/vesicle-associated membrane protein-3 (VAMP-3) in mediating endocytosis and endosomal trafficking in platelets. This v-SNARE has been reported to be localized to intracellular punctate structures within platelets.[31] Using a knockout (KO) mouse, with normal hemostasis and whose platelets had no aggregation or secretion defects,[32] we demonstrated that VAMP-3 plays a role in Fg uptake and governs platelet endocytosis. VAMP-3 deletion caused defective αIIbβ$_3$-mediated Fg uptake and accumulation, whereas fluid phase pinocytosis, as monitored by dextran uptake, was only marginally affected, both in vivo and ex vivo. Platelet spreading on Fg and thrombin-stimulated clot retraction was faster in the VAMP-3$^{-/-}$ platelets. In addition, we demonstrated that platelets sort endocytosed cargo into discrete endosomal compartments in vivo and ex vivo, and this process was defective in VAMP-3$^{-/-}$ platelets. Collectively, our work presents VAMP-3 as a regulator of platelet endocytosis, and this knockout animal model adds to the repertoire of tools for studying endocytic trafficking in platelets while maintaining normal exocytosis and hemostasis.

Methods

See supplemental Methods (available on the *Blood* Web site) for additional materials and methods.

Plate assay to measure endocytosis

Opaque/black 96-well polystyrene plates (Corning, Corning, NY) were coated with 5% bovine serum albumin in phosphate-buffered saline (PBS) overnight at room temperature (RT). Wild-type (WT) and KO washed platelets (100 μL; 5×10^7/mL), preincubated with 1 mM $CaCl_2$ for 5 minutes, were added to each well and incubated with varying concentrations of fluorescein isothiocyanate (FITC)–Fg (Invitrogen, Carlsbad, CA), low-molecular-weight (10 kDa) Oregon Green 488-Dextran (Invitrogen), or Alexa 568-Transferrin (Invitrogen) for increasing times at 37°C. Fluorescence intensities were measured using a SpectraMax plate reader (Molecular Devices, Sunnyvale, CA) before and after addition of 0.04% trypan blue (TB; 0.04% TB quenched >95% of FITC signal, Oregon Green 488 signal, and Alexa 568 signal, data not shown) to stop reactions at various times. Standard curves were generated using serial dilutions of FITC-Fg or Oregon Green 488-Dextran or Alexa 568-Transferrin.

Three-dimensional–structured (3D) illumination super-resolution microscopy

Washed WT and KO platelets (1.0×10^9/mL) were incubated ex vivo with Alexa 647-Fg and Oregon Green 488-Dextran (1 μM each) at 37°C for indicated times and then fixed with 2% paraformaldehyde (PFA). Centrifugation (700*g* for 5 minutes) was used to remove fixative, and platelet pellets were resuspended in PBS. The platelets were fixed a second time with 2% PFA and then allowed to settle onto poly-D-lysine-coated coverslips (0.1 mg/mL) for more than 90 minutes at RT in a humid chamber. To quench the fixative,

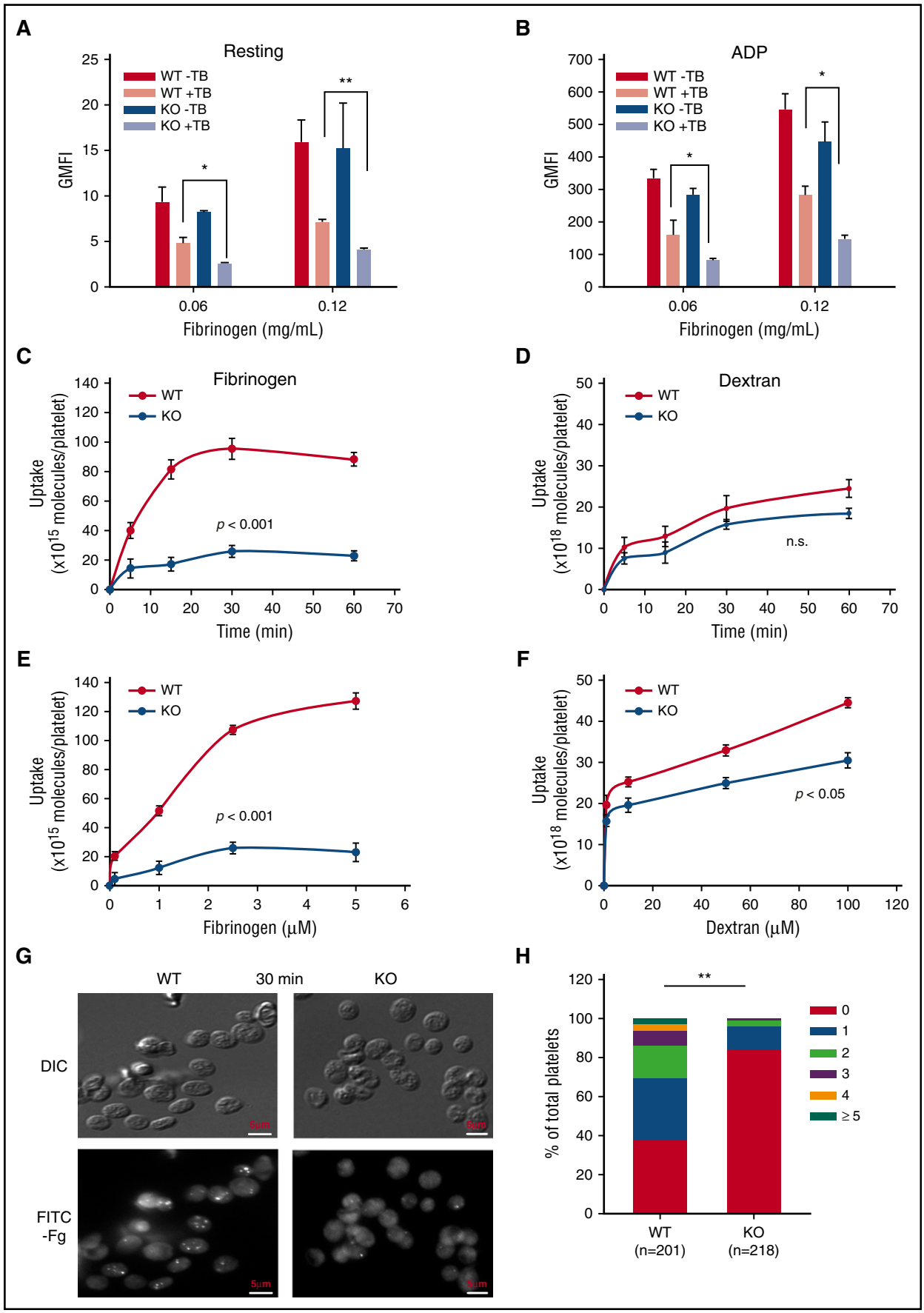

Figure 2.

coverslips were incubated cell side down in 50 mM NH_4Cl in PBS for 30 minutes at RT. Coverslips were washed with 1× PBS and mounted in Prolong Diamond Antifade Mounting medium (Invitrogen) and cured for 2 days at RT in the dark.

For in vivo experiments, 24 hours after injection of Alexa 647-Fg and Oregon Green 488-Dextran (2 μM/mouse for both fluorophores), mice were euthanized and platelets were directly fixed during the blood draw. Platelets were then isolated and allowed to settle onto poly-D-lysine-coated coverslips. Imaging was performed using the Ti-E N-STORM/N-SIM super-resolution microscope (Nikon, Melville, NY), fitted with an Apo SR 100×/1.49 NA oil-objective and A1R camera at the University of Kentucky Imaging Core. Images were processed using NIS-Elements v3.2 N-SIM/STORM software (Nikon) and Adobe Photoshop CS5 (Adobe, San Jose, CA).

Immunofluorescence microscopy

Washed WT and KO platelets (1.0×10^9/mL) were incubated ex vivo with Alexa 647-Fg and Oregon Green 488-Dextran (1 μM each) at 37°C and then fixed with 2% PFA. Centrifugation (700*g* for 5 minutes) was used to remove fixative, and platelet pellets were resuspended in PBS. The platelets were then allowed to settle onto poly-D-lysine-coated coverslips (0.1 mg/mL) and incubated overnight at 4°C. Platelets were then washed once with 1× PBS, reduced with 0.1% $NaBH_4$ for 10 minutes at RT, rewashed with 1× PBS thrice for 15 minutes each with gentle shaking, and then permeabilized for 15 minutes with 0.2% Triton X-100 in 1× PBS at RT. Cells were then blocked in 10% fetal bovine serum/0.05% Triton X-100 in 1× PBS for 90 minutes at RT, followed by incubation with primary antibodies prepared in 5% fetal bovine serum/0.05% Triton X-100 in 1× PBS overnight at 4°C. The platelets were then washed 5 times with 1× PBS for 15 minutes each and incubated with secondary antibodies in 5% fetal bovine serum/0.05% Triton X-100 in 1× PBS for 1 hour at RT. Cells were washed 5 times for 15 minutes each with 1× PBS and then postfixed with 4% PFA for 10 min. After washing in 1× PBS once, coverslips were washed and mounted in Prolong Diamond Antifade Mounting medium and cured for 2 days at RT in the dark. Imaging was performed using the Nikon Ti-E N-STORM/N-SIM super-resolution microscope, fitted with an Apo SR 100X/1.49 NA oil objective and A1R camera at the University of Kentucky Imaging Core. Images were processed using NIS-Elements v3.2 N-SIM/STORM software (Nikon) and Adobe Photoshop CS5 (Adobe). Control experiments with only secondary antibodies (but no primary antibodies) were performed to eliminate nonspecific staining artifacts from immunoglobulin G binding.

Results

VAMP-3$^{-/-}$ platelets were Fg-deficient

Given past reports of Fg endocytosis by platelets[3,10] and the intracellular localization of VAMP-3,[31] we asked whether VAMP-3 played a role in Fg uptake and/or accumulation. In Figure 1A-B, VAMP-3$^{-/-}$ platelets, isolated from 3 individual mice, had less platelet-associated Fg (~40% less; $P \leq .001$) than WT littermates, indicating a defect in uptake and/or accumulation of Fg. However, plasma Fg levels were unchanged, suggesting loss of VAMP-3 did not affect Fg production (supplemental Figure 1). The major Fg-binding integrin,[10] $\alpha IIb\beta_3$, was also unaffected by loss of VAMP-3 because β_3 levels were unchanged in the VAMP-3$^{-/-}$ platelets, as measured by western blotting (Figure 1C-D). Ligands for other platelet integrins, for example, fibronectin (binds to $\alpha_5\beta_1$ and $\alpha_v\beta_3$) and vitronectin (binds to $\alpha_v\beta_3$), were either unchanged or slightly elevated in VAMP-3$^{-/-}$ platelets (Figure 1C-D). Of note, vitronectin levels were also increased in the Arf6$^{-/-}$ platelets compared with WT.[28] Levels of other endocytic cargoes, such as VEGF and Sema3F (binds to VEGFR), were unchanged. VAMP-3 is thought to localize on both Early and Recycling endosomes.[33,34] Markers for those compartments, Rab4 (Early), Rab11 (Recycling), and Rab7 (Late endosomes), were unchanged in VAMP-3$^{-/-}$ platelets (Figure 1C-D). Other platelet endocytic markers, for example, dynamin-2, clathrin heavy chain, and disabled-2, were also unchanged (Figure 1C-D). Levels of de novo synthesized cargo, for example, platelet factor 4, and other platelet SNARE proteins were unaltered in the VAMP-3$^{-/-}$ platelets.[32] Defective Fg endocytosis did not alter the gross morphology of VAMP-3$^{-/-}$ platelets. Moreover, the VAMP-3$^{-/-}$ mice had normal platelet, red blood cell, and white blood cell counts (supplemental Table 1), although their platelet size was ~5% smaller than the platelets from age-matched littermate controls. Thus, the reduced intraplatelet Fg observed in VAMP-3$^{-/-}$ platelets was not a result of alterations in any of the endocytic proteins and regulators analyzed, or decreased levels of β_3 integrins or plasma Fg.

Reduced levels of internalized Fg could be caused by decreased surface and/or activated $\alpha IIb\beta_3$ levels. Surface levels of $\alpha IIb\beta_3$, under resting conditions, were unchanged in the VAMP-3$^{-/-}$ platelets, as measured by flow cytometry (supplemental Figure 2Ai-iii). As expected,[28] thrombin-induced activation mobilized an internal pool of $\alpha IIb\beta_3$ integrins, as indicated by the ~25% increase in the total surface $\alpha IIb\beta_3$. This ~25% increase was equally noted in both WT and VAMP-3$^{-/-}$ platelets. Similarly (supplemental Figure 2Bi-iii), levels of activated $\alpha IIb\beta_3$, as measured by Jon/A binding, were unchanged in VAMP-3$^{-/-}$ platelets, consistent with normal aggregation.[32] Defective Fg uptake, despite normal levels of $\alpha IIb\beta_3$, could be attributed to defective surface-binding of Fg to $\alpha IIb\beta_3$. Under steady-state conditions, FITC-Fg binding at 2 different concentrations (0.06 and 0.12 mg/mL) was unaffected in the VAMP-3$^{-/-}$ platelets (supplemental Figure 2C). Taken together, these results indicated that the lower Fg levels in VAMP-3$^{-/-}$ platelets were not a result of defective binding or reduced surface levels of $\alpha IIb\beta_3$, suggesting VAMP-3 plays an essential role in uptake and/or accumulation of Fg in platelets.

Fg uptake/storage was defective in VAMP-3$^{-/-}$ platelets

ADP stimulation enhances internalization of Fg-bound $\alpha IIb\beta_3$ into platelets.[20,21] We verified this observation using flow cytometry to measure FITC-Fg uptake in resting and ADP-stimulated WT and VAMP-3$^{-/-}$ platelets (Figure 2A-B). Similar to Huang et al,[28] we used

Figure 2. VAMP-3$^{-/-}$ platelets had defective fibrinogen uptake. WT and VAMP-3$^{-/-}$ platelets (1.0×10^9/mL) were kept resting (A) or stimulated with ADP (10μM) (B), then incubated with FITC-Fg (0.06 or 0.12 mg/mL) at 37°C for 30 minutes. The platelets were then put on ice for 20 minutes and fixed with 2% PFA (final concentration), and geometric mean fluorescent intensity measurements were taken by flow cytometry before and after the addition of 0.04% TB. Quantification of data shows both geometric mean fluorescence intensity measurements before addition of TB (WT/ VAMP-3$^{-/-}$–TB; dark bars), which gives the total fluorescence, and after addition of TB (WT/ VAMP-3$^{-/-}$+ TB; light bars), which gives the measure of internal fluorescence. As explained in Methods, WT and VAMP-3$^{-/-}$ platelets were added to each well in an opaque 96-well plate and either incubated with FITC-Fg (2 μM) (C) or low-molecular-weight (10 kDa) Oregon Green 488-Dextran (2 μM) (D) for times from 0 to 60 minutes at 37°C. Similarly, WT and VAMP-3$^{-/-}$ platelets were incubated with either FITC-Fg (0.1-5 μM) (E) or low-molecular-weight (10 kDa) Oregon Green 488-Dextran (1-100 μM) (F) for 30 minutes at 37°C. Reactions were stopped at given points, and fluorescence was measured before and after the addition of 0.04% TB. Data were plotted using SigmaPlot software (v13.0) and graphed as numbers of molecules of Fg or dextran endocytosed per platelet. No ADP was added to the plate assays. Statistical analyses were performed using 1-way ANOVA test; *$P \leq 0.05$; **$P \leq 0.01$; ***$P \leq .001$; n.s., not significant. (G) Washed WT and VAMP-3$^{-/-}$ platelets (1×10^9/mL) were incubated with FITC-Fg at final concentrations of 1 μM at 37°C for increasing times up to 30 minutes. Platelets were fixed with 2% PFA (final concentration) and mixed with 0.1% TB before imaging. Platelets were visualized as described in the supplemental Methods. Exposure times for DIC were 100 ms, whereas for the FITC, laser were 500 ms. Scale bars, 5 μM. (H) Quantification of the number of FITC$^+$ puncta/platelet in both WT and VAMP-3$^{-/-}$ samples were plotted using SigmaPlot software (v13.0). Statistical significance determined using Mann-Whitney *U* test; **$P \leq .01$. Data are representative of 3 independent experiments (mean ± standard error of the mean [SEM]) for all.

0.04% TB to quench external FITC fluorescence (including the fluorescence that is trapped within the open canalicular system) and measured TB-resistant fluorescence as a metric of endocytosis. Platelets were incubated with FITC-Fg, either in the presence or absence of ADP, at 37°C, and then chilled on ice to arrest further endocytosis, fixed with 2% PFA, and analyzed using flow cytometry before (darker bars) and after (lighter bars) addition of TB. In the absence of TB, geometric mean fluorescence intensity measurements represent the total fluorescence intensity of FITC-Fg present both inside and on the platelet surface. In Figure 2A, under resting conditions, the total fluorescence intensity before the addition of TB was equivalent between WT and VAMP-3$^{-/-}$ platelets, confirming equal amounts of FITC-Fg bound in each sample. Post-TB quenching, VAMP-3$^{-/-}$ platelets had ~50% less FITC-Fg signal ($P \leq .03$ at 0.06 mg/mL and $P \leq .006$ at 0.12 mg/mL), indicating that under steady-state conditions, VAMP-3 loss affected internal accumulation of Fg in platelets. In Figure 2B, ADP stimulation (10 μM) increased overall net fluorescence for both WT and VAMP-3$^{-/-}$ platelets by ~30-fold, indicative of $\alpha IIb\beta_3$ activation caused by ADP receptor signaling.[20,21] Although VAMP-3$^{-/-}$ platelets had enhanced Fg association comparable to WT, the internalized FITC-Fg pool (resistant to TB) was still less, consistent with a ~50% deficit in internalized FITC-Fg ($P \leq .039$ at 0.06 mg/mL and $P \leq .023$ at 0.12 mg/mL). Collectively, these data suggest VAMP-3 deletion leads to impaired endocytic uptake and/or accumulation of Fg into platelets in both resting and activated states.

Endocytosis defects in VAMP-3$^{-/-}$ platelets: receptor-mediated vs fluid-phase cargo

Platelets can internalize diverse cargoes; for example, vascular endothelial growth factor,[35] bacteria, viruses,[36] and so on. We asked whether VAMP-3 could be a central mediator of cargo uptake in platelets. Uptake of fluorescently tagged receptor-mediated cargo (Fg) and fluid-phase pinocytosis cargo (low-molecular-weight dextran) was tracked in a plate-based assay using TB as a quencher of external fluorescence. In Figure 2C,E, WT platelets internalized FITC-Fg in a time-dependent (up to 60 minutes) and dose-dependent (up to 5 μM) manner. VAMP-3$^{-/-}$ platelets showed a robust defect in both time- and dose-dependent Fg uptake. Arf6$^{-/-}$ platelets were also defective in FITC-Fg uptake (supplemental Figure 3A,C), confirming our earlier studies.[28] On the basis of these data, Fg internalization within WT platelets exhibited time- and dose-dependence that appeared to saturate. This is indicative of a receptor-mediated endocytosis process.

Fluid-phase endocytosis/pinocytosis was constitutive in WT platelets and showed a linear increase in dextran uptake with time (Figure 2D) and concentration (Figure 2F). Loss of VAMP-3 modestly affected dextran uptake, but there was still a time- and dose-dependence, similar to WT. Loss of Arf6 appeared to have a greater effect on fluid-phase uptake (supplemental Figure 3B,D). Our data agreed with reports of normal small-molecule pinocytosis, for example, horseradish peroxidase, in VAMP-3$^{-/-}$ mouse embryonic fibroblasts.[37,38] Interestingly, from a quantitative perspective, more dextran molecules were endocytosed than Fg (10^{18} vs 10^{15} molecules/platelet over the course of 60 minutes). These data were consistent with fluid-phase pinocytosis having a higher overall capacity than receptor-mediated uptake. Collectively, our data suggested that both VAMP-3 and Arf6 are more important for receptor-mediated uptake of Fg in platelets than for fluid-phase pinocytosis.

Low-resolution epifluorescence microscopy confirmed these results. WT and VAMP-3$^{-/-}$ platelets were incubated with 1 μM FITC-Fg for 30 minutes, fixed, treated with 0.04% TB to quench external fluorescence, and imaged by epifluorescence. WT platelets had more FITC-Fg^{+} puncta than VAMP-3$^{-/-}$ platelets after 30 minutes (Figure 2G). Quantification of total fluorescent puncta present per platelet showed that more than 80% of VAMP-3$^{-/-}$ platelets (vs ~30% in WT) had no puncta, consistent with defective Fg uptake (Figure 2H; overall $P \leq .01$). Only WT platelets had 3 or more puncta compared with 2 or fewer in VAMP-3$^{-/-}$ platelets. Cultured VAMP-3$^{-/-}$ megakaryocytes, when incubated with Alexa 647-Fg (1 μM), also showed fewer Fg^{+} puncta (60% fewer in VAMP-3$^{-/-}$ at 60 minutes; supplemental Figure 4) compared with WT, suggesting defective Fg uptake/storage in megakaryocytes as well as in platelets. Collectively, our data suggest VAMP-3 is important for fibrinogen uptake in both megakaryocytes and platelets. Consistent with our ex vivo plate-based assay that shows time-dependent uptake of dextran (Figure 2D), quantification of dextran^{+} fluorescent puncta (indicative of dextran uptake) in WT and VAMP-3$^{-/-}$ platelets at 30 minutes showed no significant differences (supplemental Figure 5A-B).

Taken together, these data show that Fg uptake and/or accumulation is dramatically reduced in the VAMP-3$^{-/-}$ platelets and comparatively more affected than dextran uptake and/or accumulation. Because $\alpha IIb\beta_3$ activation and Fg-binding to $\alpha IIb\beta_3$ remained unaffected (supplemental Figure 2), it appears that VAMP-3 could be mediating membrane trafficking steps that are downstream of Fg binding and/or internalization, yet required for Fg accumulation.

Sorting of endocytic cargo in platelets

To probe another receptor-mediated process, we examined the uptake of Alexa 568-transferrin (supplemental Figure 6). Uptake was dose- and time-dependent, as well as saturable, much like that seen with Fg (Figure 2C,E). VAMP-3$^{-/-}$ platelets showed an obvious defect, consistent with VAMP-3 (and perhaps Arf6) being more important for receptor-mediated uptake/storage of cargo than for fluid-phase pinocytosis. This is also consistent with different endocytic trafficking routes being active in platelets. To address this point, platelets were co-incubated with equimolar concentrations of Alexa 647-Fg and Oregon Green 488-Dextran and imaged by 3D-structured illumination microscopy over time. At 1 minute, Fg (magenta, Figure 3A) was found at the platelet plasma membrane (possibly bound to $\alpha IIb\beta_3$), whereas dextran (green) already was internalized into punctate structures. Surface staining for dextran was minimal, most likely because no specific dextran receptor is present on platelets. At 5 minutes, while surface staining was still visible, Fg^{+} puncta appeared, with a concomitant increase in dextran^{+} puncta. By 30 minutes, more Fg-positive puncta appeared and the surface localization was less apparent. Strikingly, Fg and dextran puncta did partially overlap (indicated by the white spots as in Figure 3A, C), suggesting the 2 cargoes might take different routes to a similar compartment. Consistently, VAMP-3$^{-/-}$ platelets had fewer Fg puncta compared with WT, whereas dextran uptake was less affected.

The accumulation of Fg and dextran in platelets was also examined in vivo. Equimolar amounts of Alexa 647-Fg and Oregon Green 488-Dextran were injected via the retro-orbital sinus of VAMP-3$^{-/-}$ mice and WT littermate controls, and platelets were harvested and imaged 24 hours postinjection. In both WT and VAMP-3$^{-/-}$ platelets, Fg and dextran were localized to distinct compartments at 24 hours (Figure 3B). VAMP-3$^{-/-}$ platelets had a robust defect in Fg accumulation with very few fluorescent puncta visible. Surprisingly, dextran^{+} puncta were also diminished in VAMP-3$^{-/-}$ platelets, suggesting that loss of VAMP-3 has a greater effect on accumulation during the longer incubation times (24 hours) than during acute uptake at shorter times. This argues that VAMP-3 is essential for both acute uptake and long-term accumulation/storage of receptor-mediated cargo (Fg), whereas it preferentially affects accumulation/storage over acute uptake of fluid-phase pinocytic cargo. The integrity of the fluorescently tagged dextran was not evaluated, so its degradation could also explain our findings.

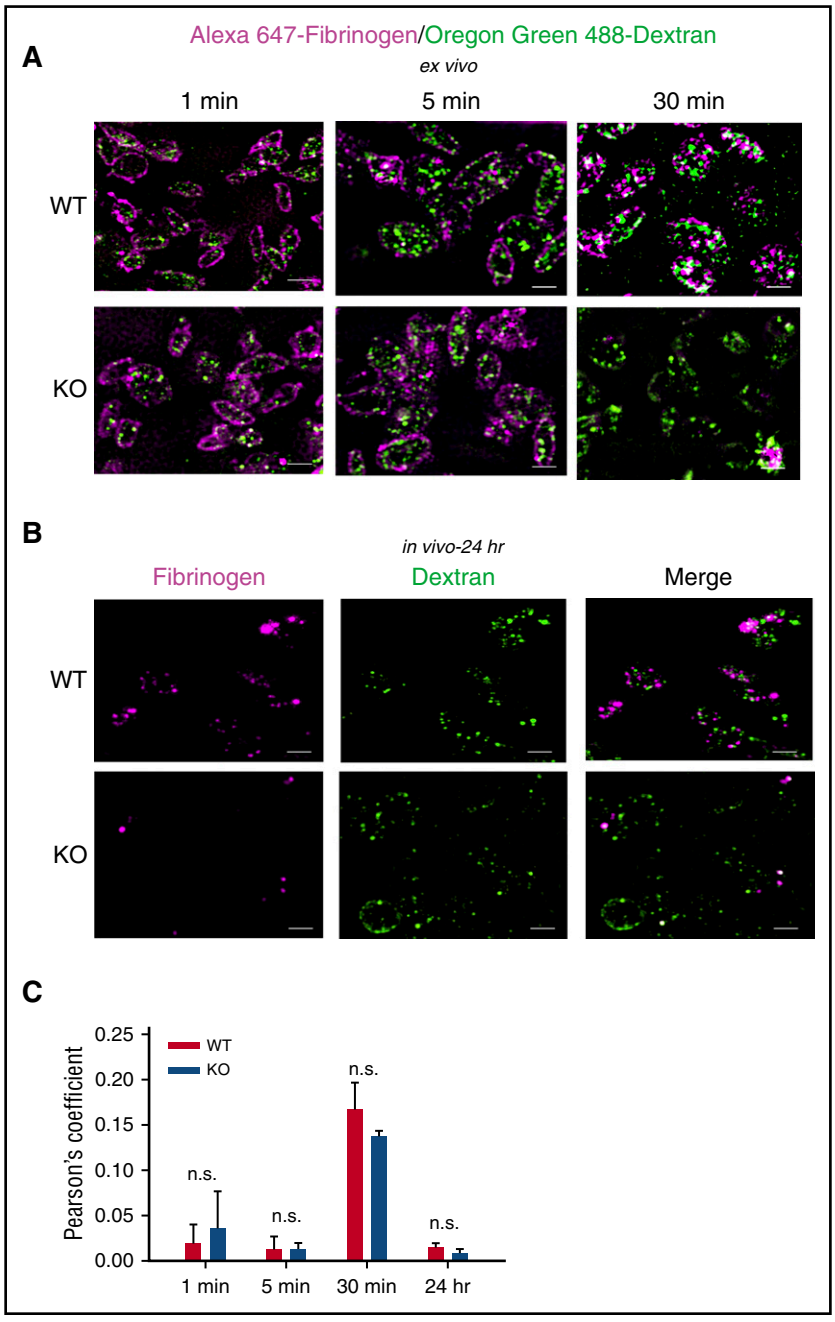

Figure 3. Receptor-mediated and fluid-phase cargoes took different endocytic routes in platelets. (A) Washed WT and VAMP-3$^{-/-}$ platelets (1.0×10^9/mL) were incubated ex vivo with Alexa 647-Fg and Oregon Green 488-Dextran at final concentrations of 1 μM each and incubated at 37°C for 1 to 30 minutes and prepared for 3D-structured illumination microscopy imaging as described in Methods. (B) WT and VAMP-3$^{-/-}$ mice were injected with Alexa 647-Fg and Oregon Green 488-Dextran at a concentration of 2 μM each per fluorophore through the retroorbital sinus. Twenty-four hours postinjection, platelets were harvested and prepared for 3D-structured illumination microscopy imaging. Slides from panels A and B were then imaged using the Nikon Ti-E N-STORM/N-SIM super-resolution microscope, and images were processed using the NIS-Elements v3.2 N-SIM/STORM suite software. Scale bars, 5 μm. Data are representative of at least 2 independent experiments. (C) Pearson's correlation coefficients were calculated using the NIS-Elements v3.2 N-SIM/STORM suite software to show overlap between Alexa 647-Fg and Oregon Green 488-Dextran (depicted in white) at the indicated points. Graph shows the mean ± SEM of 2 independent experiments, with at least 30 cells per field, taken over 3 to 4 fields per time. Statistical analyses were performed using Student *t* test; n.s., not significant.

To dissect the sorting routes present in platelets, we compared the distribution of endocytosed Fg and dextran to that of Rab4 and Rab11, markers for Early and Recycling endosomes, respectively (Figure 4). In WT platelets, both cargoes were colocalized at 30 minutes and stayed so at 60 minutes (Figures 3A and 4A-B, Ci). At 30 minutes, more of the Fg and dextran colocalized with Rab4, suggesting an Early endosome distribution (Figure 4A,Cii-iii). By 60 minutes, more of the Fg and dextran colocalized with Rab11 (and less so with Rab4), suggesting a Recycling endosome distribution (Figure 4B-Civ-v). The time-dependent transit between compartments is consistent with previous studies.[28] To examine cargo trafficking in VAMP-3$^{-/-}$ platelets, we focused on the few that were Fg^{+}. The endocytosed cargo had a distinctly different distribution. As expected, Fg levels were lower than seen in WT, and fewer platelets were positive for Fg. The little that was taken up partially colocalized with endocytosed dextran (Figure 4). The overlap between Fg and Rab4 or Rab11 was less obvious at both 30 and 60 minutes. This was also true for endocytosed dextran, suggesting loss of VAMP-3 affected the interendosomal trafficking seen in WT platelets. However, based on these altered distributions of cargoes, it is unclear which step or steps VAMP-3 mediates. In WT platelets, some of the endocytosed Fg and dextran colocalized with VWF (a marker for α-granules) as early as 30 minutes (Figure 5A-B), consistent with previous studies.[39] There was poorer colocalization of endocytosed Fg and dextran with VWF in VAMP-3$^{-/-}$ platelets, again suggesting VAMP-3 is needed for correct intercompartmental transit in platelets.

Loss of VAMP-3 affected TPOR/Mpl receptor signaling

Because VAMP-3 mediates trafficking of several transmembrane receptors, such as the transferrin receptor (supplemental Figure 6; Galli

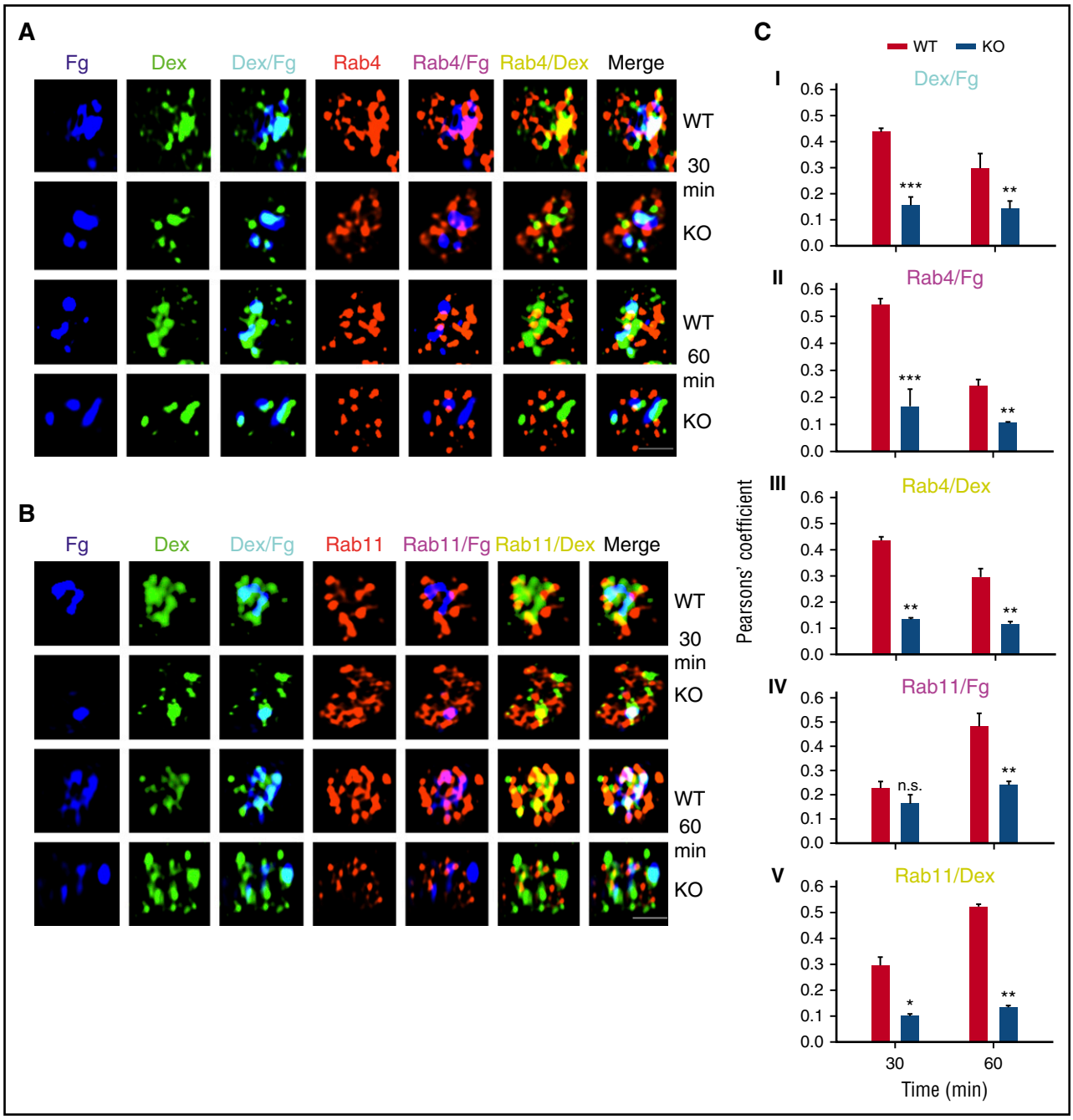

Figure 4. Loss of VAMP-3 affected transit of cargoes to endosomes. Washed platelets (1×10^9/mL) were incubated with Alexa 647-Fg and Oregon Green 488-Dextran at final concentrations of 1 μM each and incubated at 37°C for 30 to 60 minutes and prepared for immunofluorescence microscopy, as described in Methods. Platelets were incubated with anti-Rab4 rabbit polyclonal antibody (1:250 dilution) and anti-Rab11 rabbit polyclonal antibody (1:250 dilution), and then with Alexa 568-conjugated goat anti-rabbit IgG secondary antibody (1:1,000 dilution). Images were taken using the Nikon Ti-E N-STORM/N-SIM super-resolution microscope and digitally magnified by ×30. The Alexa 647-Fg signal was faux-colored blue to aid in identifying overlaps. Scale bars, 1 μm. Data are representative of 2 independent experiments. (C) Pearson's correlation coefficients were calculated using the NIS-Elements v3.2 N-SIM/STORM suite software to show overlap among (i) Alexa 647-Fg and Oregon Green 488-Dextran (depicted in cyan), (ii) Alexa 568-Rab4 and Alexa 647-Fg (depicted in magenta), (iii) Alexa 568-Rab4 and Oregon Green 488-Dextran (depicted in yellow), (iv) Alexa 568-Rab11 and Alexa 647-Fg (depicted in magenta), and (v) Alexa 568-Rab11 and Oregon Green 488-Dextran (depicted in yellow), at the indicated times. Overlap of all 3 fluorophores is depicted in white in the merge panel. Graph shows the mean ± SEM of 2 independent experiments, with at least 30 cells per field, taken over 3 to 4 fields per time. Statistical analyses were performed using Student *t* test; $^*P \leq .05$; $^{**}P \leq .01$; $^{***}P \leq .001$; n.s., not significant.

et al[40]), we asked whether other receptors rely on VAMP-3-dependent trafficking. Thrombopoietin (TPO) binding to TPO receptor (TPOR/Mpl) induces internalization of the receptor via a dynamin-2 and clathrin-mediated process that initiates Janus kinase 2 (JAK2) phosphorylation in platelets.[22,41] In contrast to dynamin-$2^{-/-}$, VAMP-$3^{-/-}$ platelets did not exhibit constitutive JAK2 phosphorylation. Instead, they showed a time-dependent increase in phospho-JAK2 similar to WT. However, at each time, phospho-JAK2 was markedly elevated in VAMP-$3^{-/-}$ (supplemental Figure 7A-B), with statistically significant differences at 15 minutes ($P \leq .05$) and at 30 minutes ($P \leq .05$). The levels of total JAK2 were lower in the VAMP-$3^{-/-}$ platelets compared

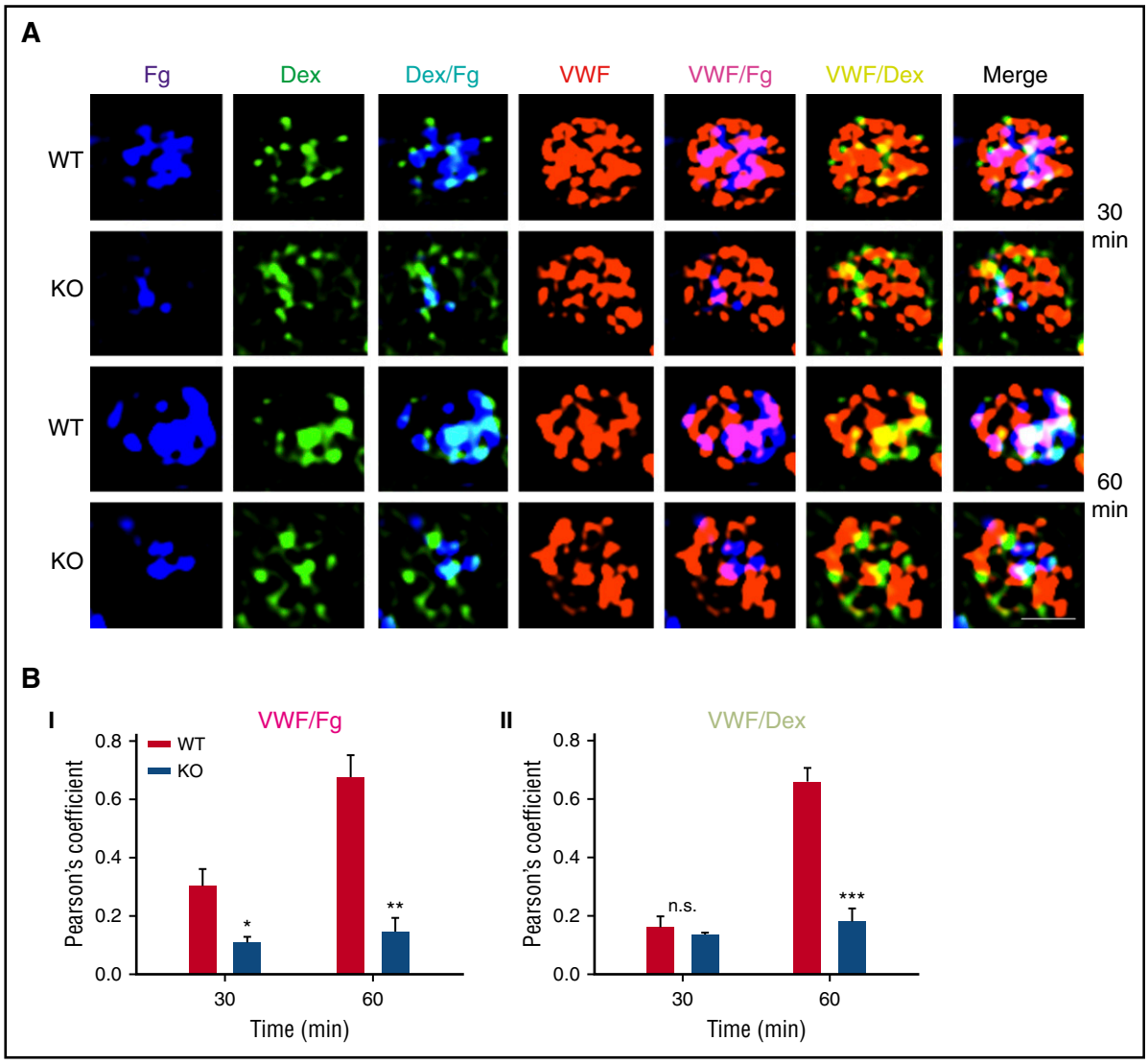

Figure 5. Loss of VAMP-3 affected transit of cargoes to α-granules. (A) Washed platelets (1×10^9/mL) were incubated with Alexa 647-Fg and Oregon green 488-Dextran at final concentrations of 1 μM each and incubated at 37°C for 30 to 60 minutes and prepared for immunofluorescence microscopy, as described in Methods. Platelets were incubated with anti-VWF rabbit polyclonal antibody (1:500 dilution) and then with Alexa 568-conjugated goat anti-rabbit immunoglobulin G secondary antibody (1:1,000 dilution). Images were taken using the Nikon Ti-E N-STORM/N-SIM super-resolution microscope, and digitally magnified by ×30. The Alexa 647-Fg signal was faux colored blue to aid in identifying overlaps. Scale bar, 1 μm. Data are representative of 2 independent experiments. (B) Pearson's correlation coefficients were calculated using the NIS-Elements v3.2 N-SIM/STORM suite software to show overlap between (i) Alexa 568-VWF and Alexa 647-Fg (depicted in magenta) and (ii) Alexa 568-VWF and Oregon Green 488-Dextran (depicted in yellow) at the indicated times. Overlap of all 3 fluorophores is depicted in white in the merge panel. Graph shows the mean ± SEM of 2 independent experiments, with at least 30 cells per field, taken over 3 to 4 fields per time. Statistical analyses were performed using Student *t* test; $^*P \leq .05$; $^{**}P \leq .01$; $^{***}P \leq .001$; n.s., not significant.

with WT, but total TPOR was unchanged (supplemental Figure 7A). Our data suggest that although TPOR levels may be unaffected, there exists a VAMP-3-mediated membrane trafficking step or steps that occurs on TPO-bound TPOR internalization and that alters JAK2 phosphorylation. We also asked whether Arf6 could play a role in signaling through the TPOR-JAK2 axis. Arf6$^{-/-}$ platelets demonstrated normal JAK2 phosphorylation on TPO induction similar to WT platelets, with no change in TPOR levels (supplemental Figure 7C-D). Arf6, thus, may be less important than VAMP-3 or dynamin-2 in regulating TPOR/Mpl-JAK2 signaling. It should be noted that loss of VAMP-3 did not affect total Arf6 levels or the rate of stimulation-dependent Arf6-GTP to Arf6-GDP transition reported by Choi et al.[42] However, there was a significant increase in basal Arf6-GTP in VAMP-3$^{-/-}$ platelets over time (supplemental Figure 8). The significance of this is unclear at present.

Loss of VAMP-3 enhanced platelet spreading and clot retraction

VAMP-3 has been shown to modulate β_1 integrin-dependent cell adhesion and migration in epithelial cell lines.[43,44] We asked whether VAMP-3 plays a similar role in $\alpha IIb\beta_3$-mediated platelet spreading. Consistent with unaltered steady-state binding to Fg (supplemental Figure 2C), there were no statistically significant differences in static adhesion to Fg by VAMP-3$^{-/-}$ platelets (Figure 6C). To determine whether VAMP-3 loss affected platelet spreading, we monitored WT and VAMP-3$^{-/-}$ platelet spreading on Fg-coated surfaces over time at 37°C. VAMP-3 deletion caused faster spreading with significantly larger platelet surface areas covered in as early as 30 minutes ($P \leq .05$; Figure 6A-B). The rate of spreading was 82% faster in the VAMP-3$^{-/-}$ platelets (rate of 0.80 μm^2/min for VAMP-3$^{-/-}$ vs 0.44 μm^2/min for WT, assuming spreading is linear over time). In similar experiments,

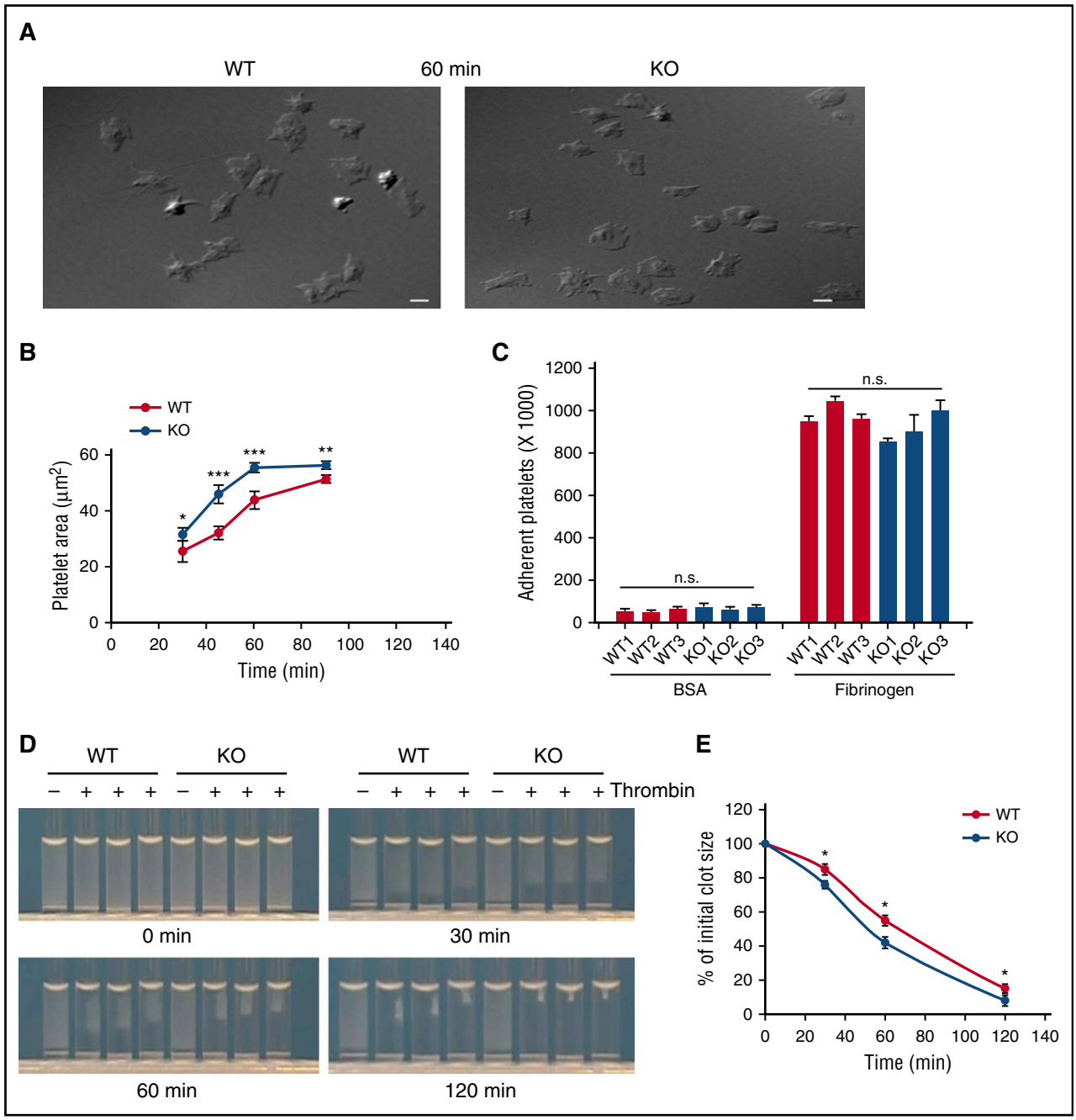

Figure 6. VAMP-3$^{-/-}$ platelets spread faster on Fg and had enhanced clot retraction. (A) Representative images of WT and VAMP-3$^{-/-}$ platelets allowed to spread on fibrinogen (50 μg/mL in 1× PBS) for 60 minutes are shown. Images of spread platelets were taken using DIC microscopy as described in supplemental Methods. Exposure times for DIC images were 100 ms. Scale bars, 5 μm. (B) Quantification of platelet surface area from WT and VAMP-3$^{-/-}$ Fg-spread platelets for indicated times. Data are representative of 2 independent experiments (mean ± SEM). (C) Quantification of static adhesion on 50 μg/mL human Fg and 5% bovine serum albumin-coated surfaces for WT and VAMP-3$^{-/-}$ calcein-labeled platelets harvested from 3 different VAMP-3$^{-/-}$ and WT mice. Adherent platelets were measured by fluorescence, using a SpectraMax plate reader. Data were plotted using SigmaPlot software (v13.0). (D) Representative images of thrombin-stimulated (0.05 U/mL; denoted by +) clot retraction in WT and VAMP-3$^{-/-}$ platelets at increasing times. (E) Clot sizes were measured, and the percentages of clot size relative to initial suspension volume (measured at time 0 and set as 100%) were determined and plotted. Three different VAMP-3$^{-/-}$ and corresponding WT littermate controls were used in this experiment. Statistical analyses were performed using the Student *t* test; *$P \leq .05$; **$P \leq .01$; ***$P \leq .001$; n.s., not significant.

VAMP-3$^{-/-}$ platelets showed a slight enhancement in spreading on fibronectin (0.0728 μm^2/min for VAMP-3$^{-/-}$ vs 0.0481 μm^2/min for WT) over time ($P \leq .01$ at 60 minutes and $P \leq .05$ at 120 minutes), but not on poly-D-lysine- or on albumin-coated coverslips (supplemental Figure 9). Consistent with increased spreading on fibrinogen, clot retraction was also faster in VAMP-3$^{-/-}$ platelets compared with WT (Figure 6D-E). Unlike spreading, which is a linear function, clot retraction proceeded exponentially over time, with the decay constant for WT being 0.011% of initial clot size/min and that for VAMP-3$^{-/-}$ 0.015% of initial clot size/min. This led to a 36% enhancement in the rate of clot retraction in the VAMP-3$^{-/-}$ platelets as early as 30 minutes ($P \leq .05$) and continued at 60 minutes ($P \leq .05$) and 120 minutes ($P \leq .05$). Exogenous Fg was added in excess and was not limiting. Thus, loss of VAMP-3 led to enhanced platelet spreading and clot

retraction. However, these alterations did not affect platelet aggregation or hemostasis, as measured by tail-bleeding assay (supplemental Figure 10; Schraw et al[32]).

Discussion

Ours is the first report that the v-SNARE, VAMP-3, is involved in internal membrane trafficking in platelets. This trafficking is needed for Fg and transferrin uptake/accumulation, platelet spreading, clot retraction, and proper regulation of TPOR signaling. Loss of VAMP-3 did not affect platelet counts or ultrastructure (supplemental Table 1; Schraw et al[32]). Static levels of total surface and activated $\alpha IIb\beta_3$ were unaltered in resting and thrombin-stimulated VAMP-3$^{-/-}$ platelets (supplemental Figure 2A-B), as was the steady-state binding of Fg (supplemental Figure 2C). We previously reported[32] that VAMP-3 played no significant role in platelet exocytosis, and its loss did not overtly affect tail-bleeding times (supplemental Figure 10). Thus, the loss of VAMP-3 had no gross effects on the platelet's role in hemostasis, despite effects on platelet spreading and clot retraction. Loss of VAMP-3 did affect Fg endocytosis, accumulation, and trafficking. We also characterized some of the routes taken by endocytosed cargo and demonstrated that VAMP-3 plays a role in at least 1 step. Given this phenotypic profile, the VAMP-3$^{-/-}$ mice described here will be valuable in determining if and how endocytosis affects platelet biology.

In this manuscript, we describe a plate-based system that allows more flexibility and more sensitivity when assaying endocytosis than flow cytometry. Using this assay, we showed that Fg and transferrin internalization reached saturation in WT platelets and demonstrated classical receptor-ligand saturation kinetics over the range of concentrations tested (Figure 2C,E; supplemental Figures 3A,C and 6). Conversely, fluid-phase pinocytosis of small molecules, that is, dextran, was constitutive, rapid, and at least 1000-fold higher in capacity than receptor-mediated Fg or transferrin uptake. This is some of the first evidence that platelets have at least 2 distinct mechanisms for taking up molecules from their surrounding microenvironment. Despite these differences in initial uptake, there is overlap in where the molecules go inside the platelet. Over time, both types of cargo colocalized, first with Rab4 and then with Rab11. At the later times, the cargoes are found colocalized with VWF, a marker for α-granules. These data confirm previous reports in which endocytosed Fg passes through Rab4$^+$ Early endosome, Rab11$^+$ Recycling endosomes, and multivesicular bodies on the way to α-granules.[28,39] VAMP-3$^{-/-}$ platelets had a robust defect in Fg and transferrin uptake/accumulation (Figures 1 and 2; supplemental Figure 6). Given the distribution of endocytosed Fg in the few Fg$^+$, VAMP-3$^{-/-}$ platelets we could find, this v-SNARE could be involved at the step mediating entry into the Rab4$^+$ compartment (Figure 4). Initial uptake of dextran was not affected by VAMP-3's loss (Figure 2D,F; supplemental Figure 5), but transit of endocytosed dextran (Figures 4 and 5) and its accumulation at longer times in vivo (24 hours) was defective (Figure 3B). These data argue that VAMP-3 is required for at least 1 endocytic step that is needed to accumulate both fluid-phase-endocytosed and receptor-mediated-endocytosed material. This step is likely where the 2 routes converge at a Rab4$^+$ compartment. Because entry to the Rab4$^+$ compartment is probably disrupted, it is difficult to assess the role of VAMP-3 in subsequent steps.

By affecting an early step in the trafficking of specific surface receptors (both liganded and empty), the loss of VAMP-3 could reroute these receptors to and from the plasma membrane. Our previous studies showed that the small GTPase Arf6 was important for Fg uptake/accumulation, integrin recycling, and some platelet functions; for example, clot retraction and spreading.[28] VAMP-3$^{-/-}$ platelets had a similar phenotype, suggesting a similar role. In epithelial cells, VAMP-3 is important for integrin-mediated migration, particularly trafficking at the lamellipodia, where VAMP-3 localizes to focal adhesions.[43] Tetanus toxin cleavage of VAMP-3 reduced migration, but enhanced adhesion to collagen, laminin, and fibronectin, perhaps because of impaired recycling of β_1 integrins.[43] In Figure 6A-B and supplemental Figure 9, the rate of platelet spreading on immobilized Fg and Fn was faster for VAMP-3$^{-/-}$ than WT platelets. This, together with the Arf6$^{-/-}$ phenotype, reinforces the notion that altered integrin trafficking affects platelet spreading. Unlike epithelial cells where migration is polarized, platelet spreading on coated coverslips occurs in all directions. If VAMP-3 controls spatially specific receptor trafficking that facilitates vectorial platelet spreading in a thrombus, its loss could make random, multidirectional fusion more efficient, leading to enhanced spreading in all directions. Although we favor this explanation because it can be applied to both VAMP-3$^{-/-}$ and Arf6$^{-/-}$ platelets,[28] there is a valid alternative. Loss of VAMP-3 could affect the formation of exocytic SNARE complexes. VAMP-3$^{-/-}$ platelets have a modest secretion rate enhancement.[32] In contrast, loss of VAMP-7, another key platelet v-SNARE, causes a defect in α-granule secretion and platelet spreading.[45] Given that VAMP-7-mediated exocytosis is important for spreading, VAMP-3-mediated enhanced secretion could enhance spreading. By reducing the levels of a potential competitive v-SNARE,[46] loss of VAMP-3 could increase the formation of other SNARE complexes (containing VAMP-7 or VAMP-8, Syntaxin-8 or Syntaxin-11, and SNAP-23), and thus increase the exocytosis events needed for spreading. Future comparisons of VAMP-3$^{-/-}$ and VAMP-7$^{-/-}$ platelets will be invaluable in understanding how endo- and exocytosis affect platelet spreading. The enhanced spreading and clot retraction phenotypes we observed are subtle and might be expected to predispose the mice toward a more prothrombotic phenotype. However, that was not obvious in the tail-bleeding or $FeCl_3$-injury models (Schraw et al[32]; supplemental Figure 10; S.J. and S.W.W., manuscript in preparation). Equally, loss of VAMP-7 had no effect on tail-bleeding and laser-induced thrombosis[45]; thus, more refined assays will be needed to parse the biological ramifications of the loss of these 2 v-SNAREs.

Platelets contain roughly 50 α-granules,[47,48] yet we did not see equivalent numbers of Fg$^+$ puncta in platelets at 30 minutes or even after the overnight incubation in vivo (Figures 2G-H, 3, 4, and 5). The global distribution of Fg into α-granules, seen in recent immunoelectron microscopy studies, would seem at odds with our data.[49] Although clearly megakaryocytes endocytose Fg (supplemental Figure 4), it is not clear whether all granules are loaded equally. At least for platelets, our observations could mean that only specific α-granules are readily loaded with endocytosed cargo during circulation. Alternatively, our data could imply that Fg loading into all α-granules requires more time, perhaps the lifetime of a platelet. It is equally possible that larger amounts of FITC-Fg are needed to fully label all the granules. Testing these possibilities will require future experiments, but will yield a more detailed understanding of α-granule biogenesis and the potential for creating heterogeneity in α-granule populations as platelets circulate.

Endocytosis is a multistage process that uses several routes of entry-transit-exit. Our data suggest that many of these paths are present and active in platelets. Clearly, VAMP-3 and Arf6 mediate some but not all the key steps that can facilitate Fg uptake/accumulation and the dynamic processes that affect contact-based signaling; that is, spreading and clot retraction. The VAMP-3-dependent and

Arf6-dependent steps seem more important for receptor-mediated endocytosis than fluid-phase uptake. Platelets do have a robust fluid-phase pinocytosis system that likely takes in a host of small molecules. Our data show that these cargoes are trafficked to distinct compartments within the platelet. Thus, endocytosis may allow platelets to actively sample their environment and perhaps interpret what they sample. The VAMP-3$^{-/-}$ mice described here and the Arf6$^{-/-}$ mice described previously[28] offer unique reagents to begin to parse the complexity of platelet endocytosis and to better define its physiological relevance.

Acknowledgments

The authors thank members of the S.W.W. laboratory (Jinchao Zhang, Smita Joshi, Thirushan Wigna-Kumar, Harry Chanzu, Laura Tichacek, and Patrick Thompson) for their careful perusal of this manuscript. The authors also thank Greg Bauman and Jennifer Strange (University of Kentucky Flow Cytometry Core Facility), and Thomas Wilkop (University of Kentucky Imaging Core Facility) for their technical assistance. Additionally, the authors thank the Department of Laboratory Animal Resources for their technical assistance.

This work is supported by grants from the National Institutes of Health, National Heart, Lung, and Blood Institute (HL56652 and HL138179), a grant from the American Heart Association Grant-in-Aid (AHA16GRNT27620001), and a Veterans Affairs Merit Award to S.W.W, and a University of Vermont REACH grant to B.A.B.

Authorship

Contribution: M.B. and S.W.W. designed and performed the experiments, analyzed data, and wrote the manuscript; S.J. performed the tail-bleeding analysis; J.Z. assisted with the Arf6 pull-down assay; C.L.M. assisted with imaging the megakaryocytes; B.A.B. performed the experiments on the megakaryocytes; and S.Y. and B.S. assisted with the super-resolution microscopy analysis.

Conflict-of-interest disclosure: The authors declare no competing financial interests.

ORCID profiles: M.B., 0000-0002-5139-5861; S.J., 0000-0001-6925-2116; J.Z., 0000-0002-7514-6624; S.W.W., 0000-0001-5577-0473.

Correspondence: Sidney W. Whiteheart, Department of Molecular and Cellular Biochemistry, University of Kentucky College of Medicine, B271 BBSRB, 741 S Limestone, Lexington, KY 40536; e-mail: whitehe@uky.edu.

References

1. Joshi S, Whiteheart SW. The nuts and bolts of the platelet release reaction. *Platelets*. 2017;28(2):129-137.
2. Zucker-Franklin D. Endocytosis by human platelets: metabolic and freeze-fracture studies. *J Cell Biol*. 1981;91(3 Pt 1):706-715.
3. Harrison P, Wilbourn B, Debili N, et al. Uptake of plasma fibrinogen into the alpha granules of human megakaryocytes and platelets. *J Clin Invest*. 1989;84(4):1320-1324.
4. Klement GL, Yip TT, Cassiola F, et al. Platelets actively sequester angiogenesis regulators. *Blood*. 2009;113(12):2835-2842.
5. Banerjee M, Whiteheart SW. The ins and outs of endocytic trafficking in platelet functions. *Curr Opin Hematol*. 2017;24(5):467-474.
6. Morgenstern E. Coated membranes in blood platelets. *Eur J Cell Biol*. 1982;26(2):315-318.
7. Klinger MH, Klüter H. Immunocytochemical colocalization of adhesive proteins with clathrin in human blood platelets: further evidence for coated vesicle-mediated transport of von Willebrand factor, fibrinogen and fibronectin. *Cell Tissue Res*. 1995;279(3):453-457.
8. Handagama PJ, Bainton DF. Incorporation of a circulating protein into alpha granules of megakaryocytes. *Blood Cells*. 1989;15(1):59-72.
9. Handagama PJ, Shuman MA, Bainton DF. Incorporation of intravenously injected albumin, immunoglobulin G, and fibrinogen in guinea pig megakaryocyte granules. *J Clin Invest*. 1989;84(1):73-82.
10. Handagama P, Scarborough RM, Shuman MA, Bainton DF. Endocytosis of fibrinogen into megakaryocyte and platelet alpha-granules is mediated by alpha IIb beta 3 (glycoprotein IIb-IIIa). *Blood*. 1993;82(1):135-138.
11. Wencel-Drake JD, Painter RG, Zimmerman TS, Ginsberg MH. Ultrastructural localization of human platelet thrombospondin, fibrinogen, fibronectin, and von Willebrand factor in frozen thin section. *Blood*. 1985;65(4):929-938.
12. Behnke O. Degrading and non-degrading pathways in fluid-phase (non-adsorptive) endocytosis in human blood platelets. *J Submicrosc Cytol Pathol*. 1992;24(2):169-178.
13. Wencel-Drake JD. Plasma membrane GPIIb/IIIa. Evidence for a cycling receptor pool. *Am J Pathol*. 1990;136(1):61-70.
14. Wencel-Drake JD, Frelinger AL III, Dieter MG, Lam SC. Arg-Gly-Asp-dependent occupancy of GPIIb/IIIa by applaggin: evidence for internalization and cycling of a platelet integrin. *Blood*. 1993;81(1):62-69.
15. Wencel-Drake JD, Plow EF, Zimmerman TS, Painter RG, Ginsberg MH. Immunofluorescent localization of adhesive glycoproteins in resting and thrombin-stimulated platelets. *Am J Pathol*. 1984;115(2):156-164.
16. Michelson AD, Adelman B, Barnard MR, Carroll E, Handin RI. Platelet storage results in a redistribution of glycoprotein Ib molecules. Evidence for a large intraplatelet pool of glycoprotein Ib. *J Clin Invest*. 1988;81(6):1734-1740.
17. Lorenz V, Stegner D, Stritt S, et al. Targeted downregulation of platelet CLEC-2 occurs through Syk-independent internalization. *Blood*. 2015;125(26):4069-4077.
18. Nisar SP, Cunningham M, Saxena K, Pope RJ, Kelly E, Mundell SJ. Arrestin scaffolds NHERF1 to the P2Y12 receptor to regulate receptor internalization. *J Biol Chem*. 2012;287(29):24505-24515.
19. Michelson AD, Wencel-Drake JD, Kestin AS, Barnard MR. Platelet activation results in a redistribution of glycoprotein IV (CD36). *Arterioscler Thromb*. 1994;14(7):1193-1201.
20. Schober JM, Lam SC, Wencel-Drake JD. Effect of cellular and receptor activation on the extent of integrin alphaIIbbeta3 internalization. *J Thromb Haemost*. 2003;1(11):2404-2410.
21. Belitser N, Anischuk M, Veklich Y, Pozdnjakova T, Gorkun O. Fibrinogen internalization by ADP-stimulated blood platelets. Ultrastructural studies with fibrinogen-colloidal gold probes. *Thromb Res*. 1993;69(5):413-424.
22. Bender M, Giannini S, Grozovsky R, et al. Dynamin 2-dependent endocytosis is required for normal megakaryocyte development in mice. *Blood*. 2015;125(6):1014-1024.
23. Reems JA, Wang W, Tsubata K, et al. Dynamin 3 participates in the growth and development of megakaryocytes. *Exp Hematol*. 2008;36(12):1714-1727.
24. Nürnberg ST, Rendon A, Smethurst PA, et al; HaemGen Consortium. A GWAS sequence variant for platelet volume marks an alternative DNM3 promoter in megakaryocytes near a MEIS1 binding site. *Blood*. 2012;120(24):4859-4868.
25. Koseoglu S, Dilks JR, Peters CG, et al. Dynamin-related protein-1 controls fusion pore dynamics during platelet granule exocytosis. *Arterioscler Thromb Vasc Biol*. 2013;33(3):481-488.
26. Tsai HJ, Huang CL, Chang YW, et al. Disabled-2 is required for efficient hemostasis and platelet activation by thrombin in mice. *Arterioscler Thromb Vasc Biol*. 2014;34(11):2404-2412.
27. Huang CL, Cheng JC, Stern A, Hsieh JT, Liao CH, Tseng CP. Disabled-2 is a novel alphaIIb-integrin-binding protein that negatively regulates platelet-fibrinogen interactions and platelet aggregation. *J Cell Sci*. 2006;119(Pt 21):4420-4430.
28. Huang Y, Joshi S, Xiang B, et al. Arf6 controls platelet spreading and clot retraction via integrin αIIbβ3 trafficking. *Blood*. 2016;127(11):1459-1467.
29. Rowley JW, Oler AJ, Tolley ND, et al. Genome-wide RNA-seq analysis of human and mouse platelet transcriptomes. *Blood*. 2011;118(14):e101-e111.
30. Burkhart JM, Vaudel M, Gambaryan S, et al. The first comprehensive and quantitative analysis of human platelet protein composition allows the

comparative analysis of structural and functional pathways. *Blood*. 2012;120(15):e73-e82.

31. Bernstein AM, Whiteheart SW. Identification of a cellubrevin/vesicle associated membrane protein 3 homologue in human platelets. *Blood*. 1999; 93(2):571-579.
32. Schraw TD, Rutledge TW, Crawford GL, et al. Granule stores from cellubrevin/VAMP-3 null mouse platelets exhibit normal stimulus-induced release. *Blood*. 2003;102(5):1716-1722.
33. Mallard F, Tang BL, Galli T, et al. Early/recycling endosomes-to-TGN transport involves two SNARE complexes and a Rab6 isoform. *J Cell Biol*. 2002;156(4):653-664.
34. Daro E, van der Sluijs P, Galli T, Mellman I. Rab4 and cellubrevin define different early endosome populations on the pathway of transferrin receptor recycling. *Proc Natl Acad Sci USA*. 1996;93(18): 9559-9564.
35. Feng W, Madajka M, Kerr BA, Mahabeleshwar GH, Whiteheart SW, Byzova TV. A novel role for platelet secretion in angiogenesis: mediating bone marrow-derived cell mobilization and homing. *Blood*. 2011;117(14):3893-3902.
36. Youssefian T, Drouin A, Massé JM, Guichard J, Cramer EM. Host defense role of platelets: engulfment of HIV and Staphylococcus aureus occurs in a specific subcellular compartment and is enhanced by platelet activation. *Blood*. 2002; 99(11):4021-4029.
37. Allen LA, Yang C, Pessin JE. Rate and extent of phagocytosis in macrophages lacking vamp3. *J Leukoc Biol*. 2002;72(1):217-221.
38. Yang C, Mora S, Ryder JW, et al. VAMP3 null mice display normal constitutive, insulin- and exercise-regulated vesicle trafficking. *Mol Cell Biol*. 2001;21(5):1573-1580.
39. Heijnen HF, Debili N, Vainchencker W, Breton-Gorius J, Geuze HJ, Sixma JJ. Multivesicular bodies are an intermediate stage in the formation of platelet alpha-granules. *Blood*. 1998;91(7): 2313-2325.
40. Galli T, Chilcote T, Mundigl O, Binz T, Niemann H, De Camilli P. Tetanus toxin-mediated cleavage of cellubrevin impairs exocytosis of transferrin receptor-containing vesicles in CHO cells. *J Cell Biol*. 1994;125(5):1015-1024.
41. Drachman JG, Griffin JD, Kaushansky K. The c-Mpl ligand (thrombopoietin) stimulates tyrosine phosphorylation of Jak2, Shc, and c-Mpl. *J Biol Chem*. 1995;270(10):4979-4982.
42. Choi W, Karim ZA, Whiteheart SW. Arf6 plays an early role in platelet activation by collagen and convulxin. *Blood*. 2006;107(8):3145-3152.
43. Proux-Gillardeaux V, Gavard J, Irinopoulou T, Mège RM, Galli T. Tetanus neurotoxin-mediated cleavage of cellubrevin impairs epithelial cell migration and integrin-dependent cell adhesion. *Proc Natl Acad Sci USA*. 2005;102(18): 6362-6367.
44. Tayeb MA, Skalski M, Cha MC, Kean MJ, Scaife M, Coppolino MG. Inhibition of SNARE-mediated membrane traffic impairs cell migration. *Exp Cell Res*. 2005;305(1):63-73.
45. Koseoglu S, Peters CG, Fitch-Tewfik JL, et al. VAMP-7 links granule exocytosis to actin reorganization during platelet activation. *Blood*. 2015;126(5):651-660.
46. Varlamov O, Volchuk A, Rahimian V, et al. i-SNAREs: inhibitory SNAREs that fine-tune the specificity of membrane fusion. *J Cell Biol*. 2004;164(1):79-88.
47. Sixma JJ, Slot JW, Geuze HJ. Immunocytochemical localization of platelet granule proteins. *Methods Enzymol*. 1989;169: 301-311.
48. Sehgal S, Storrie B. Evidence that differential packaging of the major platelet granule proteins von Willebrand factor and fibrinogen can support their differential release. *J Thromb Haemost*. 2007;5(10): 2009-2016.
49. Pokrovskaya ID, Aronova MA, Kamykowski JA, et al. STEM tomography reveals that the canalicular system and α-granules remain separate compartments during early secretion stages in blood platelets. *J Thromb Haemost*. 2016;14(3):572-584.